Electrochemical Behavior of Single-Walled Carbon Nanotube Supercapacitors under Compressive Stress

Xin Li, Jiepeng Rong, and Bingqing Wei*

Department of Mechanical Engineering, University of Delaware, Newark, Delaware 19716

ABSTRACT The effect of compressive stress on the electrochemical behavior of flexible supercapacitors assembled with single-walled carbon nanotube (SWNT) film electrodes and 1 M aqueous electrolytes with different anions and cations were thoroughly investigated. The under-pressed capacitive and resistive features of the supercapacitors were studied by means of cyclic voltammetry measurements and electrochemical impedance analysis. The results demonstrated that the specific capacitance increased first and saturated in corresponding decreases of the series resistance, the charge-transfer resistance, and the Warburg diffusion resistance under an increased pressure from 0 to 1723.96 kPa. Wettability as well as ion-size effect of different aqueous electrolytes played important roles to determine the pressure dependence behavior of the suerpcapacitors under an applied pressure. An improved high-frequency capacitive response with 1172 Hz knee frequency, which is significantly higher compared to reported values, was observed under the compressive pressure of 1723.96 kPa, indicating an improving and excellent high-power capability of the supercapacitors under the pressure. The experimental results and the thorough analysis described in this work not only provide fundamental insight of pressure effects on supercapacitors but also give an important guideline for future design of next generation flexible/stretchable supercapacitors for industrial and consumer applications.

KEYWORDS: single-walled carbon nanotube · supercapacitor · pressure effect · impedance analysis · knee frequency · ion-size effect.

One of the biggest challenges that we are facing today is to find and use an alternative energy to replace the fossil fuel-based energy sources. Although renewable energy technologies, such as wind turbines, solar cells, and hydropower, can provide sufficient energy production, there is an urgent need for finding and optimizing efficient energy storage devices that can harness the alternative energy produced. For small scale energy storage devices which require a higher power density and longer cycle lifetime, supercapacitors or electrical double-layer capacitors (EDLCs)[1,2] outweigh rechargeable batteries, albeit the fact that batteries normally hold a higher energy density. Recently, with the development of lightweight, flexible, and wearable-electronic devices,[3−5] a newly indispensable requirement is raised for the energy storage devices to be also flexible and/or stretchable, which brings intensive research across the industries and academia.[6−9]

Carbon nanotubes[10−16] and their composite materials[17,18] have been extensively investigated as promising electrode materials for supercapacitors over the past decade because of their unique structures,[19] excellent electrical conductivity,[20] and large specific surface area.[21] Most recently, in order to meet the needs for power supply of flexible electronic devices, there is a strong interest in employing single-walled carbon nanotubes (SWNTs)[22,23] or their composites[24,25] to make flexible/stretchable supercapacitors. Fundamental understanding of the ambient condition effects, such as temperature[26] and electrolyte,[27,28] on the electrochemical performance of the supercapacitors has been investigated. However, the effect of mechanically compressive stress, one of the most influential factors on the electrochemical performance of the SWNT flexible/stretchable supercapacitors, has not been tackled in the open literature. The establishment and understanding of correlation between the optimal applied pressure and the different electrolyte ions on the electrochemical performance are extremely crucial to fully utilize the potential of the assembled flexible supercapacitors and to predict their durability. It will also provide an important guidance for the packaging process.

In this study, we have investigated the effect of compressive pressure between two SWNT electrodes on the electrochemical performance of the flexible supercapacitors laminated in a plastic package with a variety of aqueous electrolyte solutions.

*Address correspondence to weib@udel.edu.

Received for review July 9, 2010 and accepted September 01, 2010.

Published online September 9, 2010. 10.1021/nn101595y

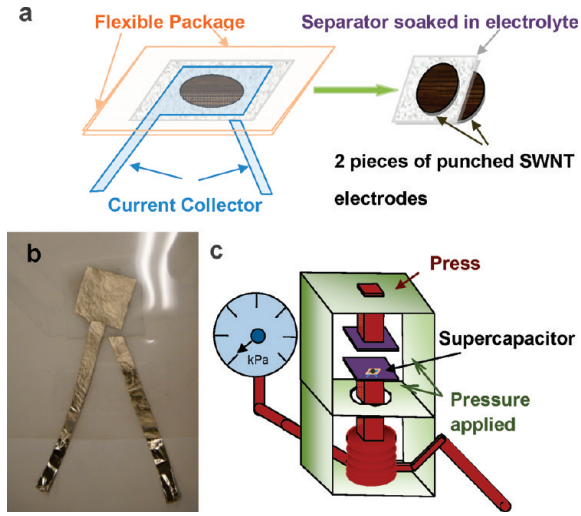

Figure 1. (a) Schematic of supercapacitor assembly with SWNT electrodes. (b) Digital camera image of an assembled flexible supercapacitor.(c) Schematic of pressure applied facility on a supercapacitor.

An aqueous electrolyte generally provides a high-energy and -power density for supercapacitors and is expected to respond quickly under a mechanical pressure, meeting the demands of the flexible/stretchable electronic devices when they require an instant high-power input. The correlation between the applied pressure and the different electrolyte ions as well as its corresponding electrochemical performance is thoroughly investigated for providing a guideline for proper usage and package design of next generation flexible/stretchable supercapacitors.

RESULTS AND DISCUSSION

Figure 1 shows the schematics of an SWNT flexible supercapacitor assembly and pressure test (detailed information can be found in the Methods Section). After assembling the supercapacitor in the transparent package (Figure 1b), the initial pressure between the electrodes was considered to be zero when analyzing the pressure effect. Thus, only the postapplied pressure from the hydraulic press was taken into account during the experiments. Figure 2 shows scanning electron microscopy (SEM) images of the SWNT films, which present typical bundle structures with a uniform network. A high-resolution image of Figure 2b illustrates that a large majority of the SWNT bundles have average diameters of about 20 nm. It also clearly shows that most of the iron catalyst and amorphous carbon were eliminated from the SWNT films after the purification treatment.[26] The SWNT film demonstrates structural combination of a mesoporous and macroporous material, which allows aqueous-based electrolyte ions to penetrate inside the film to fully utilize all the effective surface area for establishing double-layer capacitance between the SWNT and the aqueous electrolytes. Compared with nanoporous carbon materials, counterions are expected to easily and quickly reside at the SWNT

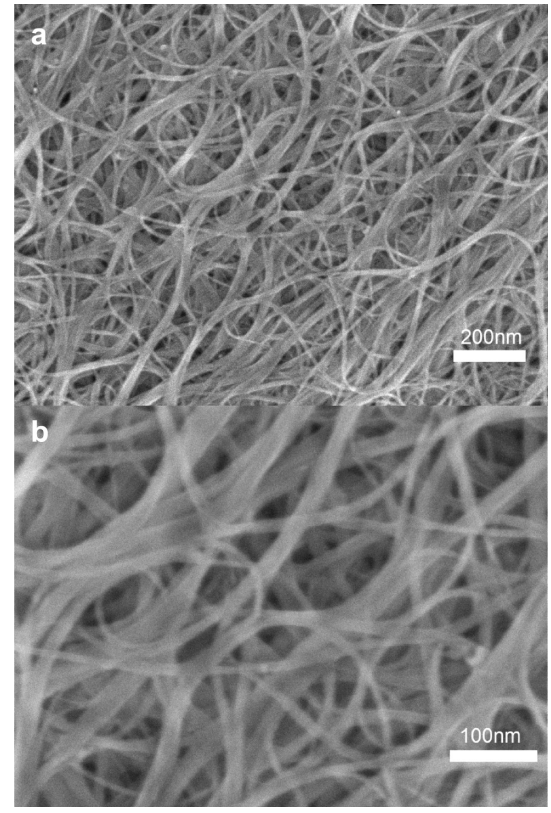

Figure 2. SEM micrograph of the SWNT film electrode as prepared by chemical vapor deposition. The electrode consists of a randomly entangled bundle structure: under (a) low and (b) high magnification.

electrode−electrolyte interface without having to enter the pores, leading to an exohedral supercapacitor with a higher power density feature.[29]

Figure 3 shows the specific capacitance values of the capacitors obtained from the voltammograms measured (Figure 4) at increasing pressures with 1 M different aqueous electrolytes, which are separated into two groups based on their pressure dependence performance. For group A electrolytes with hydrated hydroxy anions (OH^-), namely LiOH, NaOH, and KOH (Figure 3a), the initial specific capacitance is all extremely low (LiOH, NaOH, and KOH is 2.7, 3.7, and 3.6 F g^{-1}, respectively) under a pressure of 2.55 kPa. In addition, they showed a quick increase before reaching a saturation stage at a pressure of approximately 70 kPa and saturated with the stable specific capacitance value in a sequence of LiOH (25.0) > NaOH (19.7) > KOH (17.4 F g^{-1}) under a pressure of 1723.96 kPa. In contrast, for group B electrolytes with hydrated chloride (Cl^-) and nitrate (NO_3^-) anions (Figure 3b), the initial specific capacitance is much higher (LiCl, NaCl, KCl, and KNO_3 is 28, 14.9, 14.9, and 19.7 F g^{-1}, respectively) under a pressure of 2.55 kPa. Moreover, the specific capacitance values are more stable with increasing pressure compared to those with OH^- anions. Under a pressure of 1723.96 kPa, the capacitances of group B are in a sequence of LiCl (41.4) > KNO_3 (21.4) >

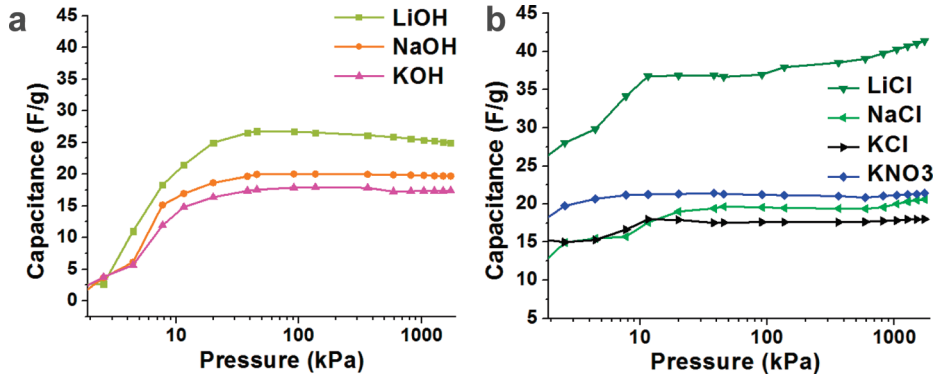

Figure 3. Specific capacitance increase trend under pressure effect for electrolytes: (a) LiOH, NaOH, and KOH. (b) LiCl, NaCl, KCl, and KNO_3.

NaCl(20.6) > KCl (18.0 F g^{-1}), showing a similar sequence as group A in terms of cations. It is also noticed that with same cation (K^+), the capacitance values are in a sequence of KNO_3 (21.4) > KCl (18.0) > KOH (17.4 F g^{-1}).

The reasons for these results are attributed to the different interfacial wettability of solutions at the electrode−electrolyte interface caused by different ions as well as the size differences among the hydrated ions. Surface wettability was first under close scrutiny as one important aspect for governing the supercapacitor performance.[16] In order to accurately evaluate the surface wettability of the different electrolytes on the SWNT films, the contact angle of each electrolyte was measured by goniometer, and the results are shown in Table 1.

It is well-known that the surface tensions of solution (γ_{soln}) and water (γ_{H_2O}) hold the following equation:[30]

$$\gamma_{soln} - \gamma_{H_2O} = gm_a \quad (1)$$

where m_a is the molar concentration of the anions (the role of cations is not significant, as confirmed from our contact angle results), and g is the slope, which can be calculated by eq 2:

$$g = a + (bz/r_a) \quad (2)$$

where z is charge of the anion and r_a is the radius of the anion (Å) and a and b are coefficients. The slope (g) of related anions has been studied by Abramzon *et al.*,[31] as shown in Table 2.

The numerical value of surface tension in terms of anions indicates OH^- > Cl^- > NO_3^- are in good agreement with the experimental data from the contact angle measurements. It is also in correlation with the specific capacitance of different electrolytes under an increasing pressure. For instance, an electrolyte with OH^- anions has the largest contact angle, indicating a poorer surface wettability compared to electrolytes with Cl^- and NO_3^- anions and resulting in a lower specific capacitance under the same pressure (Figure 3).

For electrolytes with same anions, *e.g.*, OH^- or Cl^-, the contact angle as well as the surface tension is relatively the same, however, there are still differences among the electrolytes in terms of capacitive behavior, where hydrated ion size (namely hydrated Li^+, Na^+, and K^+) of the electrolytes becomes the dominating factor after the surface wettability property. For exohedral supercapacitors, the counterions are accumulated in the double layer mainly by electrostatic forces at the distance of outer Helmholtz plane.[12,29] Theoretically, the higher the surface area is and the higher the amount of the charged ions that can access to the electrode−electrolyte interface, the higher capacitance value the supercapacitor has.[16] For aqueous electrolytes, the hydrated ion sizes can simply be estimated with eq 3:

$$d_{ion} = 0.1376 + 1.0167r_p \quad (3)$$

where d_{ion} is the average distance between ions and the nearest water molecules, and r_p is the Pauling ionic radii (Table 3). The hydrated ion size is determined by the diameter of the ion, which should be $2d_{ion}$.

Table 3 shows that with the decrease of the ion size (K^+ > Na^+ > Li^+) the capacitance will increase due to the straightforward reason that more charged cations can access to the electrode−electrolyte interface and contribute to the charge storage. This phenomenon is experimentally proved by the specific capacitance values under the saturation stage, after the surface wettability is improved by the compressive pressure applied on the supercapacitors, in both electrolytes with OH^- (Figure 3a) and Cl^- (Figure 3b) anions.

The surface wettability effect determined by anions and the ion-size effect determined by cations on the capacitive performance of the SWNT supercapacitors are evidenced by the CV curves, as shown in Figure 4. Figure 4a−g displays the CV curves of 1 M LiOH, NaOH, KOH, LiCl, NaCl, KCl, and KNO_3 aqueous electrolytes under different pressures, respectively. The initially poor wettability of electrolytes with OH^- anions was evidenced by the distorted CV curves and the low capacitance values under pressure below approximately 70

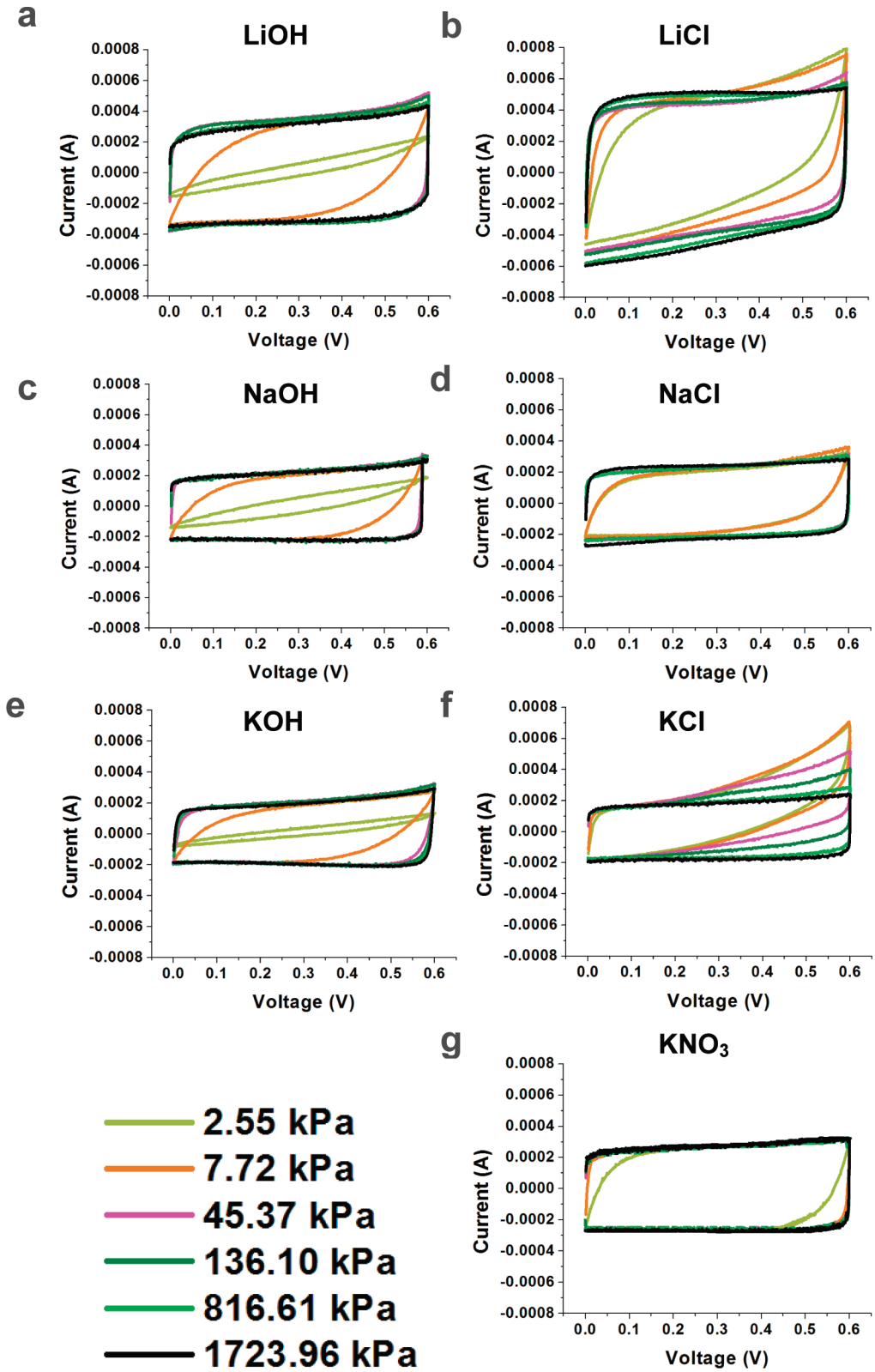

Figure 4. Cyclic voltammetry at 50 mV s^{-1} of the SWNT supercapacitors with 1 M electrolyte under increasing applied pressure (kPa): (a) LiOH, (b) LiCl, (c) NaOH, (d) NaCl, (e) KOH, (f) KCl, and (g) KNO_3.

kPa, as shown in Figure 4a, c, and e. However, for electrolytes with Cl^- and NO_3^- anions, which have a better wettability, the CV curves showed less distortion with relatively larger areas than those with OH^- anions under the same pressure. The ion-size effect on the capacitance can be recognized by comparing the loop areas in Figure 4a, c, and e (for LiOH, NaOH, and KOH) and in Figure 4b, d, and f (for LiCl, NaCl, and KCl). It was also

TABLE 1. Contact Angle of Different 1 M Electrolyte on the Surface of SWNT Electrode

electrolyte	contact angle (°)	electrolyte	contact angle (°)
KOH	60	LiOH	60
KCl	54	NaOH	60
KNO_3	45	Water	36

evidenced that the compressive pressure improves the surface wettability for all electrolytes, especially for electrolytes with OH^- anions. CV curves under pressures above approximately 70 kPa are close to a rectangular shape for all electrolytes, indicating the capacitors are approaching an ideal capacitive behavior. The compressive pressure-induced phenomenon can be further explained in detail by the electrochemical impedance spectroscopy (EIS) measurements presented below.

The primary objective of the EIS measurements is to gain insight into the pressure dependence of the capacitive and resistive elements and their effects on the performance of the supercapacitors. Figures 5 and 6 show the impedance results of Nyquist spectra in the frequency range from 100 kHz to 10 mHz measured at an equilibrium open circuit potential (~0 V) under small and large compressive pressures (Figures 5 and 6, respectively) for different electrolytes. The Nyquist spectrum can be well represented by an equivalent circuit as shown in Figure 7a. The first intersection point on the real axis of the Nyquist spectrum in the high-frequency region provides the value of the electrolyte resistance, the intrinsic resistance of the active electrode material, and the contact resistance at the interface of active material/current collector, defined as series resistance R_s.[32] The R_s element is in series with the electrical double-layer capacitance at the interface of electrode and electrolyte C_{DL}[1]. C_{DL} is in parallel with the charge-transfer resistance R_{ct} and the Warburg impedance W_o. R_{ct}, shown as the second intersection point of the semicircle on the real axis, represents the total resistance at the interface between the electrode and the electrolyte.[33] It should be noted that throughout the experiments, the current collector (Ni foils) and the SWNT electrode materials were well attached together following the same manner. It is speculated that the variation of the contact resistance between the Ni foil and the SWNT film with respect to the pressure change was the same; all the variation associated with the impedance variation should be attributed to the intrinsic difference of each electrolyte and the properties of electrode−electrolyte interface.

TABLE 2. Slope of the Surface Tension Equation

anion	g (mNm^{-1} kg · mol^{-1})
OH^-	2.00
Cl^-	1.57
NO_3^-	1.23

TABLE 3. Pauling Ionic Radii, Hydrated Ion Size, and Capacitance under 1723.96 kPa

cation	r_p (nm)	$2d_{ion}$ (nm)	capacitance with OH^- anions F g^{-1}	with Cl^- anions F g^{-1}
Li^+	0.060	0.397	25.0	41.4
Na^+	0.095	0.468	19.7	20.6
K^+	0.133	0.546	17.4	18.0

Typically, the Nyquist spectrum is divided into two regions by the knee frequency,[10,34,35] where the high-frequency semicircle is attributed to the charge-transfer process occurring at the electrode−electrolyte interface,[36] and the low-frequency curve with its slope gradually changing from 45° to 90° represents the Warburg finite-length diffusion stage when ions diffuse within the electrode.[37] Experimental results show that the knee frequency increases with the applied pressure for all electrolytes, as summarized in Table 4.

Table 4 shows that the knee frequency increase caused by the applied pressure presents a significant high frequency of 1172 Hz for all electrolytes under the maximum pressure at 1723.96 kPa. This value suggests that under the pressure the electrical energy can be stored in the double-layer capacitor at a frequency up to 1172 Hz, significantly higher than reported supercapacitors assembled with other electrode materials (a few Hz to 300 Hz),[12,34,35] indicating an excellent high-power capability. The high knee frequency could be from the pressured induced easy accessibility of ions at the electrolyte−electrode interface and the excellent electric conductivity from the SWNT films. It is noted that the semicircle in the high-frequency region (Figure 6) almost disappeared under a pressure higher than 816.61 kPa. The absence of the semicircle in the complex impedance plane implies a very good ionic conductivity at the electrode−electrolyte interface.[38,39]

Figure 7 shows pressure dependence of all the curve fitting values of R_S, R_{CT}, C_{DL}, W_{oR}, and W_{oT} of the experimental impedance spectra based upon the proposed equivalent circuit (Figure 7a). During the initial stage with a relatively low applied pressure, it is interesting to notice that the charge-transfer resistance of all the electrolytes with OH^- anions is 10-fold higher than that of the electrolytes with Cl^- or NO_3^- anions. As the charge-transfer resistance decreased with gradual pressure increase, the specific capacitance increased in all electrolytes. However, the decreasing scale for the OH^- electrolytes is much more significant than that of Cl^- or KNO_3^-. This is due to the much improved surface wettability, in consistence with the CV curves in Figure 4. For instance, the charge-transfer resistance decreases from 1550 to 270 Ω (by 82%) for LiOH electrolyte when the applied pressure increases from 2.55 to 7.72 kPa, resulting in the sharp increase of the specific capacitance from 2.66 to 18.31 F g^{-1} (under a pressure of 2.55 and 7.72 kPa, respectively). While the charge-transfer resis-

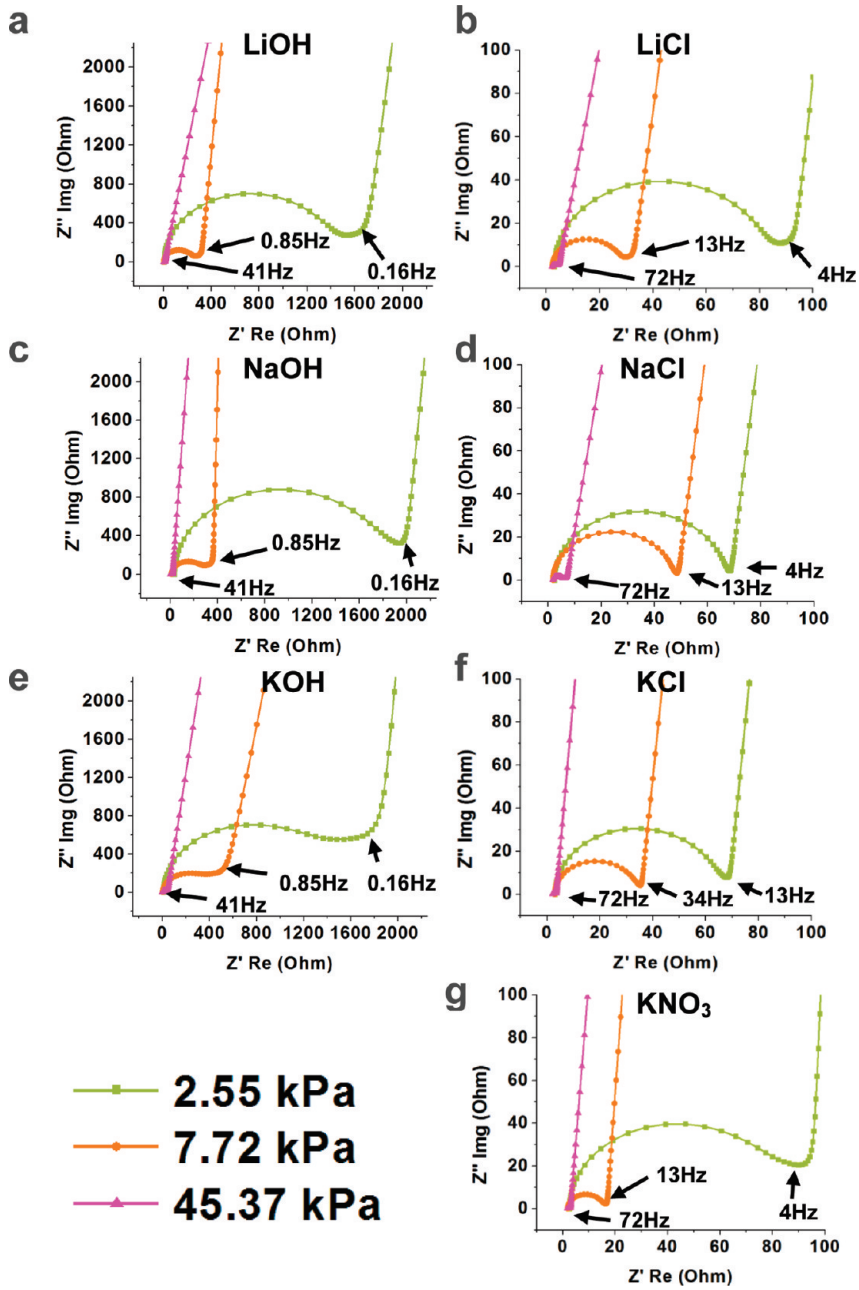

Figure 5. Impedance results with knee frequency of the SWNT supercapacitors under small applied pressures: (a) LiOH (b) LiCl (c) NaOH (d) NaCl (e) KOH (f) KCl, and (g) KNO_3.

tance decreases by 65% from 85 to 30 Ω for the LiCl electrolyte under the same applied pressures, this results in the specific capacitance increase from 28.03 to 34.15 F g^{-1} (under a pressure of 2.55 and 7.72 kPa, respectively). When a large pressure is applied, all dominant factors to determine capacitance (series, charge-transfer, and Warburg diffusion resistances) reach a relatively stable stage (saturation stage) for all electrolytes. Little improvement on the decrease of the charge-transfer resistance (Figure 7c) cannot bring much ameliorative effect to improve the specific capacitance.

In addition, the pressure increase greatly reduces the Warburg diffusion resistance (W_{oR}) and Warburg time constant (W_{oT}), especially for group A electrolytes, as shown in Figures 7d and e, respectively. The initial value of Warburg diffusion resistance is extremely large, indicating difficult ion diffusion within the electrode. In general, the ions diffuse easier and quicker into the SWNT electrode materials with better surface wettability Cl^- and NO_3^- electrolytes than that of the poor surface wettability OH^- anions electrolyte.

For the applied pressures above approximately 70 kPa, the impedance and CV curves as well as the specific capacitance change little in the supercapacitors using SWNT electrodes. This phenomenon is different from that using other pore-structured electrode materials, such as activated carbon fibers, where the specific capacitances continuously in-

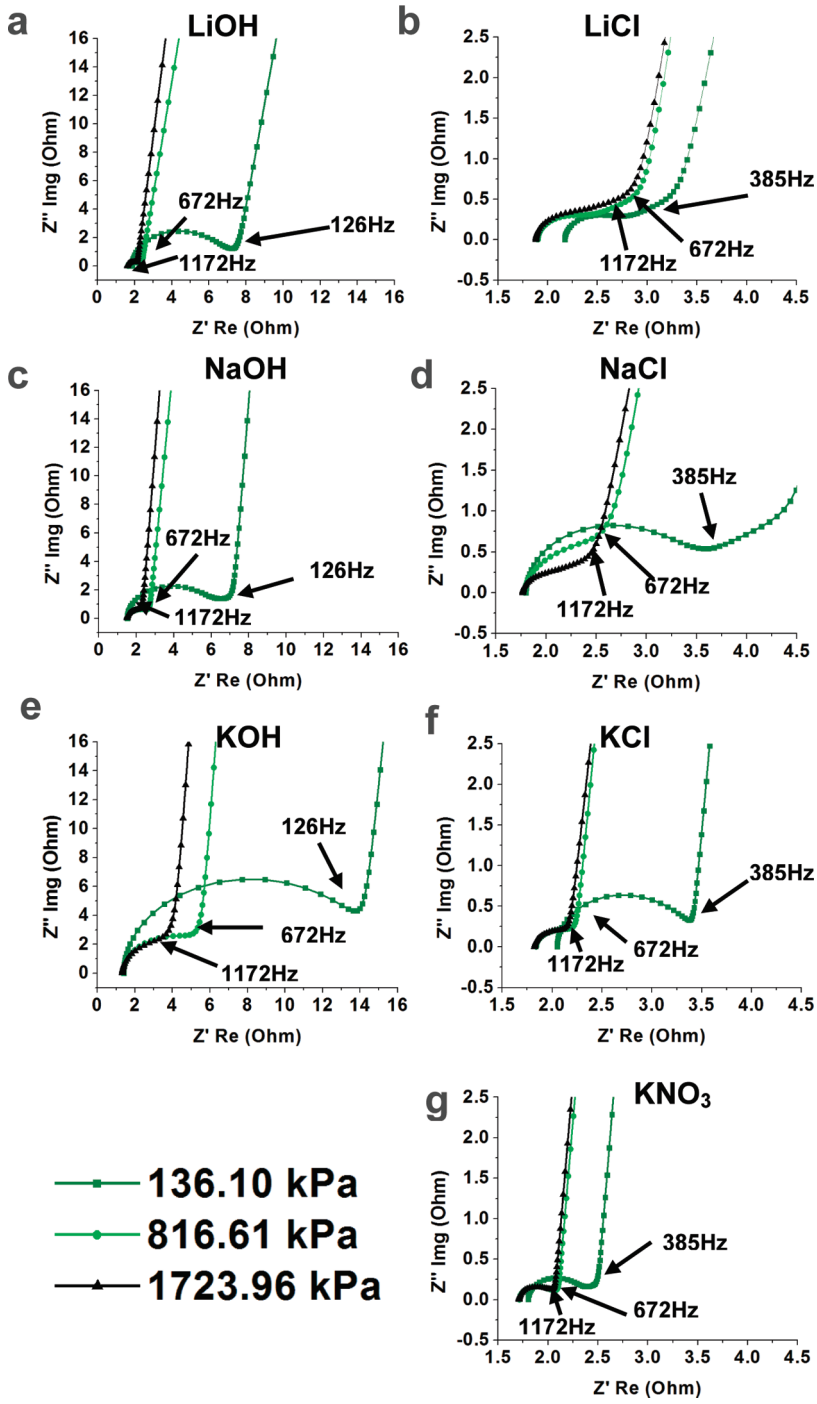

Figure 6. Impedance results with knee frequency of the SWNT supercapacitors under large applied pressures: (a) LiOH (b) LiCl(c) NaOH (d) NaCl (e) KOH (f) KCl, and (g) KNO_3.

crease even up to 2068.43 kPa, revealing that SWNTs distinguish themselves from typical microporous structured materials when they are utilized as electrode materials for supercapacitors.

In the current experiments, the different pressure dependence behavior of the quick capacitance saturation for group B electrolytes (with Cl^- or NO_3^- anions) and the drastic capacitance increase for group A electrolytes (with OH^- anions), before reaching the critical pressure around 70 kPa, can be visually explained using the schematic shown in Figure 8. The schematic illustrates the difference of groups A and B electrolytes under small and large applied pressures. To begin with a low-pressure (less than approximately 70 kPa) circumstance, the anions as well as the cations are not stabilized well within the Helmholtz layer at the electrode−electrolyte interface due to the poor wettability for the group A electrolytes with OH^- anions (Figure 8a). Most of the charged anions and cations are freely floating inside the aqueous electrolyte without

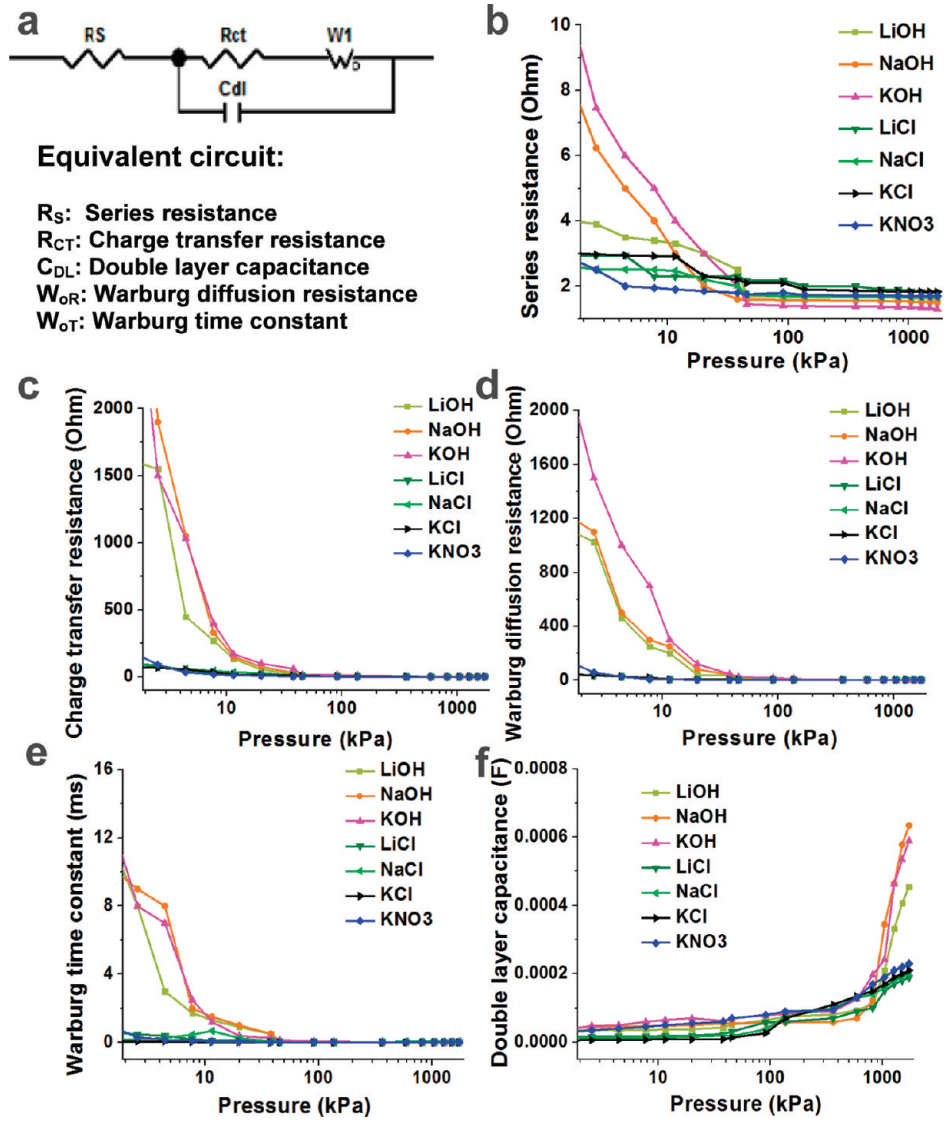

Figure 7. Impedance curve fitting results for each element in equivalent circuit: (a) AC impedance equivalent circuit, (b) series Resistance, (c) charge-transfer resistance, (d) Warburg diffusion resistance, (e) Warburg time constant, and (f) double-layer capacitance.

getting well attached to the surface of the SWNT electrodes. In contrast, the anions (Cl^- and NO_3^-) and cations from group B (Figure 8b) are more affinitive to the surface of the SWNT electrodes due to a better surface wettability (confirmed by the contact angle measurements), thus bringing a much lower initial charge-transfer resistance and a higher specific capacitance than their counterparts from group A. In terms of the ion-size effect, it is well understood that smaller cations (Li^+) take less space when residing on the electrode surface and bring a much higher specific capacitance than larger size cations (Na^+ and K^+).

This study clearly presents that SWNT electrodes are excellent materials for flexible supercapacitors and can withstand pressures as high as 1723.96 kPa, while still performing well within the cell package. It also shows the importance of the applied pressure between the SWNT electrodes and its critical influence on the properties of electrolyte anions and cations, which play governing roles in terms of the surface wettability, impedance behavior, and specific capacitance as well as the high-power capability for rapid charge/discharge of supercapacitors. The results derived from the pressure-dependent measurements on SWNT electrode supercapacitors can have a potential impact on supercapacitor assembly and packaging. They provide valuable infor-

TABLE 4. Knee Frequency (Experiment Data) vs Pressure

	knee frequency (Hz)						
pressure (kPa)	LiOH	NaOH	KOH	LiCl	NaCl	KCl	KNO_3
2.55	0.16	0.16	0.16	4	4	13	4
7.72	0.85	0.85	0.85	13	13	34	13
45.37	41	41	41	72	72	72	72
136.10	126	126	126	385	385	385	385
816.61	672	672	672	672	672	672	672
1723.96	1172	1172	1172	1172	1172	1172	1172

mation on electrode material selection and on electrolytes with suitable cation and anion properties in order to achieve the optimized capacitor performance with minimal resources, especially for perspective flexible/stretchable supercapacitors, where the pressure variation between the electrodes will be unavoidable. The variation in capacitance of a flexible supercapacitor, with the application of any deformation in usage, can then be understood with the knowledge of either an increase or decrease in the pressure between the electrodes as a result of deformation. In addition, the stability of the electrode material is of great importance to maintain stable electrochemical performance with varying applied strains in a flexible supercapacitor.

CONCLUSIONS

In summary, pressure dependence between the electrodes on the electrochemical performance of the flexible supercapacitors assembled with single-walled carbon nanotube (SWNT) electrodes in various aqueous electrolytes has been demonstrated. The specific capacitance increases in various scale with the increase of pressure depending on electrolytes. For the supercapacitors with hydrated hydroxyl anions (OH^-), the capacitance drastically increased until reaching a saturation stage due to an improved surface wettability of the electrolytes on the SWNT electrodes. For the supercapacitors with hydrated chloride (Cl^-) and nitrate (NO_3^-) anions, the capacitance saturated earlier due to the better surface wettability. Smaller ion-size cation leads to a higher specific capacitance, indicating that the ion-size effect plays an important role to determine the specific capacitance. In addition, the increased pressure also brings an improving effect on the knee frequency, which makes the flexible supercapacitor capable of storing electrical energy at significantly higher frequencies up to 1172 Hz. The fundamental understanding of the research work therefore demonstrates the ameliorative effect of compressive pressure on the SWNTs supercapacitors and provides guidelines for future design of next generation flexible/stretchable supercapacitors.

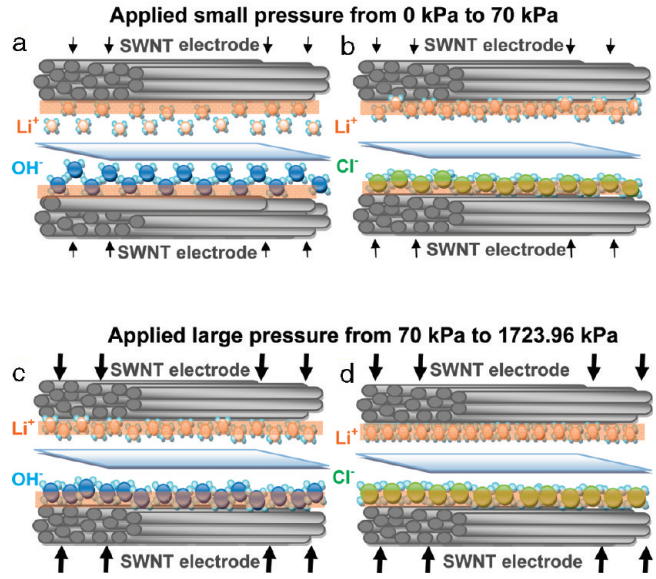

Figure 8. Schematic representation of the cations/anions in aqueous electrolyte−SWNT electrode interface during the pressure increase process with Helmholtz planes presented by the semitransparent orange band: (a) LiOH and (b) LiCl under small pressure and (c) LiOH and (d) LiCl under large pressure.

METHODS

Fabrication of the SWNT Macrofilm Electrodes. The freestanding SWNTs macrofilms were fabricated in our lab using a facile chemical vapor deposition (CVD) technique in a tube furnace.[40] A mixture of ferrocene as carbon feedstock/catalyst and sulfur as an additive to promote SWNTs growth at an atomic ratio of Fe:S = 10:1 was heated (1140 °C), while a mixture of argon and hydrogen (1500 and 150 mL min^{-1}, respectively) gas flow was input into the tube furnace. After 50−70 min reaction, the furnace was cooled to room temperature. The freestanding SWNT macrofilms were then collected from the two ends of the furnace. In order to eliminate the contamination, such as amorphous carbon and the catalytic iron particle, the as-deposited SWNT macrofilms were heat treated in the air at 440 °C for 30 min and then rinsed with diluted hydrochloric acid for 8 h. This purification procedure also significantly increased the number of functional groups (*e.g.*, O = C−OH) within the films. After the acid-wash step, SWNT films were thoroughly washed with DI water. After drying the films in the air for 8 h, two 0.5 in. diameter electrodes were punched with an arch punch. The typical weight of the SWNT electrode is about 0.5 mg. The surface morphology of the SWNT electrode was analyzed by a JEOL JSM-7400F scanning electron microscope (SEM). It is important to note that the functionalized SWNT film electrodes can be made without using binding materials, which always brings impurities into the electrodes and degrades capacitor performance. The freestanding electrodes have smooth surfaces, uniform thicknesses, and good mechanical strength. They are flexible and can be easily bent and rolled to meet the requirements for flexible supercapacitors.

Supercapacitor Assembly. The flexible supercapacitor was assembled in a plastic package. A Whatman glass microfiber filter was used as the separator between the two SWNT electrodes. In order to establish the correlation between the applied pressure and the different electrolyte ions, 1 M aqueous solutions of LiOH, NaOH, KOH, LiCl, NaCl, KCl, and KNO_3 were used as electrolytes, respectively. As shown in the schematic of Figure 1a, the supercapacitors were assembled by placing the sandwich-structured core components of a pair of SWNT electrodes separated by the aqueous electrolyte soaked separator. Nickel foils were cut to suit the shape of the core components as the current collectors, which were connected to the testing system under the circumstances of the differently applied pressures to perform a real time measurement of the electrochemical performance of the SWNTs supercapacitor. The flexible supercapacitor was sealed in a transparent plastic package with a hot press, in order to prevent potential leakage of the electrolyte. Figure 1b shows the digital camera image of the flexible supercapacitor.

Electrochemical Measurements. The electrochemical characterization under different compressive pressure was done by measuring the cyclic voltammograms (CV) and electrochemical impedance spectra (EIS). The compressive pressure between the electrodes of the SWNT supercapacitors was carefully varied in a controlled manner from 0 to 1723.96 kPa using a Carver hydraulic press. The assembled flexible SWNT supercapacitor was placed in between the parallel plates of the press, as shown in Figure 1c. At each applied pressure, the electrochemical cyclic

voltammetry and the impedance spectroscopy were characterized with an ET&G PARSTAT 2273 potentiostat/galvanostat. The values of the specific capacitance were calculated using the following equation:

$$C = \frac{A}{f \times v \times m}$$

where C is the specific capacitance, A is the integral areas of the cyclic voltammogram loops, f is the scan rate (50 mV s^{-1}), v is the voltage window (0.6 V), and m is the mass of one SWNT electrode. The AC impedance measurements were performed in the frequency range from 100 kHz to 10 mHz. All measurements were made under ambient atmospheric conditions and at room temperature. In order to obtain the equivalent circuit parameters of SWNT supercapacitors, the curve fitting of impedance expression was performed using the EIS data fitting program ZVIEW.

Contact Angle Measurements. Contact angle measurements were performed using a Rame-Hart Goniometer (model 100-00-115) at room temperature and under atmosphere pressure. Drops of aqueous electrolyte were placed on the surface of the SWNT films (same as the electrode materials) to determine the wetting characteristics.

Acknowledgment. The authors would like to thank Ryan Lewis for assistance in electrochemical measurements and Wenwen Liu for helping with contact angle measurements. The research was financially supported by the National Science Foundation CMMI-0824790.

REFERENCES AND NOTES

1. Conway, B. E. *Electrochemical Supercapacitors: Scientific Fundamentals and Technological Applications*; Kluwer Academic and Plenum: New York, 1999.
2. Simon, P.; Gogotsi, Y. Materials for Electrochemical Capacitors. *Nat. Mater.* **2008**, *7*, 845–854.
3. Lu, X. M.; Xia, Y. N. Electronic Materials: Buckling down for Flexible Electronics. *Nat. Nanotechnol.* **2006**, *1*, 163–164.
4. Sun, Y. G.; Rogers, J. A. Inorganic Semiconductors for Flexible Electronics. *Adv. Mater.* **2007**, *19*, 1897–1916.
5. Kim, D. H.; Ahn, J. H.; Choi, W. M.; Kim, H. S.; Kim, T. H.; Song, J. Z.; Huang, Y.G. Y.; Liu, Z. J.; Lu, C.; Rogers, J.A.]?>. Stretchable and Foldable Silicon Integrated Circuits. *Science* **2008**, *320*, 507–511.
6. Futaba, D. N.; Hata K.; Yamada T.; Hiraoka T.; Hayamizu Y.; Kakudate Y.; Tanaike O.; Hatori H.; Yumura M.; Iijima S. Shape-Engineerable and Highly Densely Packed Single-Walled Carbon Nanotubes and Their Application as Super-Capacitor Electrodes. *Nature* **2006**, *5*, 987−994.
7. Pushaparaj, V. L.; Shaijumon, M. M.; Kumar, A.; Murugesan, S.; Ci, L.; Vajtai, R.; Linhardt, R. J.; Nalamasu, O.; Ajayan, P. M. Flexible Energy Storage Devices Based on Nanocomposite Paper. *Proc. Natl. Acad. Sci. U.S.A.* **2007**, *104*, 13574–13577.
8. Kaempgen, M.; Chan, C. K.; Ma, J.; Chi, Y.; Gruner, G. Printable Thin Film Supercapacitors Using Single-Walled Carbon Nanotubes. *Nano Lett.* **2009**, *9*, 1872–1876.
9. Hu, L. B.; Pasta, M; La Mantia, F; et al. Stretchable, Porous, and Conductive Energy Textiles. *Nano Lett.* **2010**, *10*, 708–714.
10. Niu, C; Sichel, e.K; Hoch, R; Moy, D.; Tennent, H. High Power Electrochemical Capacitors Based On Carbon Nanotube Electrodes. *Appl. Phys. Lett.* **1997**, *70*, 1480–1482.
11. Liu, C.; Bard, A. J.; Wudl, F.; Weitz, I.; Heath, J. R. Electrochemical Characterization of Films of Single-Walled Carbon Nanotubes and Their Possible Application in Supercapacitors. *Electrochem. Solid-State Lett.* **1999**, *2*, 577.
12. Frackowiak, E.; Beguin, F. Carbon Materials for the Electrochemical Storage of Energy in Capacitors. *Carbon* **2001**, *39*, 937.
13. An, K. H.; Kim, W. S.; Park, Y. S.; Moon, J. M.; Bae, D. J.; Lim, S. C.; Lee, Y. S.; Lee, Y. H. Electrochemical Properties of High-Power Supercapacitors Using Single-Walled Carbon Nanotube Electrodes. *Adv. Funct. Mater.* **2001**, *11*, 387–392.
14. Frackowiak, E.; Jurewicz, K.; Delpeux, S.; Beguin, F. Nanotubular Materials for Supercapacitors. *J. Power Sources* **2001**, *97*, 822–825.
15. Chen, J. H.; Li, W. Z.; Wang, D. Z.; Yang, S. X.; Wen, J. G.; Ren, Z. F. Electrochemical Characterization of Carbon Nanotubes as Electrode in Electrochemical Double-Layer Capacitors. *Carbon* **2002**, *40*, 1193–1197.
16. Frackowiak, E.; Beguin, F. Electrochemical Storage of Energy in Carbon Nanotubes and Nanostructured Carbons. *Carbon* **2002**, *40*, 1775.
17. Sarico, A. S.; Bruce, P.; Scrosati, B.; Schalkwijk, W. V. Nanostructured Materials for Advanced Energy Conversion and Storage Devices. *Nat. Mater.* **2005**, *4*, 366–377.
18. Subramanian, V.; Zhu, H. W.; Wei, B. Q. Synthesis and Electrochemical Characterizations of Amorphous Manganese Oxide and Single Walled Carbon Nanotube Composites as Supercapacitor Electrode Materials. *Electrochem. Commun.* **2006**, *8*, 827–832.
19. Wei, B. Q.; Valtai, R.; Jung, Y.; Ward, J.; Zhang, R.; Ramanath, G.; Ajayan, P. M. Organized Assembly of Carbon Nanotubes. *Nature* **2002**, *416*, 295–496.
20. Wei, B. Q.; Vajtal, R.; Ajayan, R. M. Reliability and Current Carrying Capacity of Carbon Nanotubes. *Appl. Phys. Lett.* **2001**, *79*, 1172–1174.
21. Peigney, A; Laurent, Ch; Flahaut, E; Bacsa, R. R.; Rousset, A. Specific Surface Area of Carbon Nanotubes and Bundles of Carbon Nanotubes. *Carbon* **2001**, *39*, 507–514.
22. Yu, C. J.; Masarapu, C.; Rong, J. P.; et al. Stretchable Supercapacitors Based on Buckled Single-Walled Carbon Nanotube Macrofilms. *Adv. Mater.* **2009**, *21*, 4793–4797.
23. Chen, J.; Minett, A. I.; Liu, Y.; Lynam, C.; Sherrell, P.; Wang, C.; Wallace, G. G. Direct Growth of Flexible Carbon Nanotube Electrodes. *Adv. Mater.* **2008**, *20*, 566–570.
24. Meng, C. Z.; Liu, C. H.; Fan, S. S. Flexible Carbon Nanotube/Polyaniline Paper-like Films and Their Enhanced Electrochemical Properties. *Electrochem. Commun.* **2009**, *11*, 186–189.
25. Choua, S. L.; Wang, J. Z.; Chewa, S. Y.; Liua, H. K.; Doua, S. X. Electrodeposition of MnO_2 Nanowires on Carbon Nanotube Paper as Free-Standing, Flexible Electrode for Supercapacitors. *Electrochem. Commun.* **2008**, *10*, 1724–1727.
26. Masarapu, C.; Zeng, H. F.; Hung, K. H.; Wei, B. Q. Effect of Temperature on the Capacitance of Carbon Nanotube Supercapacitors. *ACS Nano* **2009**, *3*, 2199–2206.
27. Barisci, J. N.; Wallace, G. G.; Baughman, R. H. Electrochemcial Studies of Single-Wall Carbon Nanotubes in Aqueous Solutions. *J. Electroanal. Chem.* **2000**, *488*, 92–98.
28. Shiraishi, S.; Kurihara, H.; Okabe, K.; Hulicova, D.; Oya, A. Electrical Double Layer Capacitance of Highly Pure Single Walled Carbon Nanotubes (hipco Buckytubes) in Propylene Carbonate Electrolytes. *Electrochem. Commun.* **2002**, *4*, 593–598.
29. Huang, J. S.; Sumpter, B. G.; Meunier, V. A Universal Model for Nanoporous Carbon Supercapacitors Applicable to Diverse Pore Regimes, Carbon Materials, and Electrolytes. *Chem.—Eur. J.* **2008**, *14*, 6614–6626.
30. Horvath, A. L. *Handbook of Aqueous Electrolyte Solutions: Physical Properties, Estimation and Correlation Methods*; Ellis Horwood Limited: U.K., 1985.
31. Abramzon, A. A.; Kol'tsov, S. I.; Murashev, I. A. Surface Tension of Aqueous Solutions of Inorganic Salts. *Russ. J. Phys. Chem.* **1982**, *56*, 86–89.
32. Wu, Q. F.; He, K. X.; Mi, H. Y.; Zhang, X. G. Electrochemical Capacitance of Polypyrrole Nanowire Prepared by Using Cetyltrimethylammonium Bromide (CTAB) as Soft Template. *Mater. Chem. Phys.* **2007**, *101*, 367–371.
33. Yuan, C. Z.; Zhang, X. G.; Wu, Q. F.; Gao, B. Effect of temperature on the hybrid supercapacitor based on NiO and activated carbon with alkaline polymer gel electrolyte. *Solid State Ionics* **2006**, *177*, 1237–1242.
34. Hu, C. C.; Wang, C. C. Nanostructures and Capacitive Characteristics of Hydrous Manganese Oxide Prepared by

Electrochemical Deposition. *J. Electrochem. Soc.* **2003**, *150*, A1079–A1084.
35. Brevnov, D. A.; Olson, T. S. Double-layer capacitors composed of interconnected silver particles and with a high-frequency response. *Electrochim. Acta* **2006**, *51*, 1172–1177.
36. Gamby, J.; Taberna, P. L.; Simon, P.; Fauvarque, J. F.; Chesneau, M. Studies and Characterisations of various activated carbons used for carbon/carbon supercapacitors. *J. Power Source* **2001**, *101*, 109–116.
37. Sugimoto, W.; Yokoshima, K; Murakami, Y.; Takasu, Y. Charge storage mechanism of nanostructured anhydrous and hydrous ruthenium-based oxides. *Electrochim. Acta* **2006**, *52*, 1742–1748.
38. Chmiola, J.; Yushin, G.; Gogotsi, Y.; Portet, C.; Simon, P.; Taberna, P. L. Anomalous Increase in Carbon Capacitance at Pore Sizes Less than 1 Nanometer. *Science* **2006**, *313*, 1760–1763.
39. Lin, R.; Taberna, P. L.; Chmiola, L.; Guay, D.; Gogotsi, Y.; Simon, P. Microelectrode Study of Pore Size, Ion Size, and Solvent Effects on the Charge/Discharge Behavior of Microporous Carbons for Electrical Double-Layer Capacitors. *J. Electrochem. Soc.* **2009**, *156*, A7–A12.
40. Zhu, H. W.; Wei, B. Q. Direct Fabrication of Single-Walled Carbon Nanotube Macro-Films on Flexible Substrates. *Chem. Commun.* **2007**, *29*, 3042–3044.